Image restoration from noisy incomplete frequency data by alternative iteration scheme

Jijun Liu

School of Mathematics

Southeast University, Nanjing, P.R.China

The Hong Kong University of Science and Technology, May 20-24, 2019

This is a joint work with Ph.D Xiaoman Liu

Outline

1. Introduction
2. The multi-penalty regularization modeling
3. The alternative iteration scheme
4. Convergence property of iteration process
5. Numerical experiments
6. Summary

Outline

1 Introduction

2 The multi-penalty regularization modeling

3 The alternative iteration scheme

4 Convergence property of iteration process

5 Numerical experiments

6 Summary

Introduction

(a) exact image

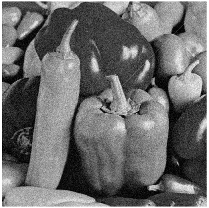

(b) Gaussian noise

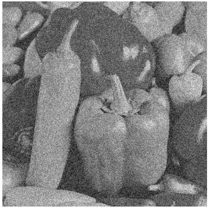

(c) 50% random noise

(d) exact color image

(e) salt pepper noise

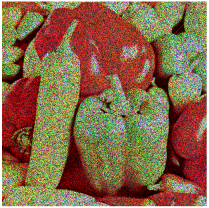

(f) speckle noise

Figure 1: Exact image and noisy images with different noise.

Introduction

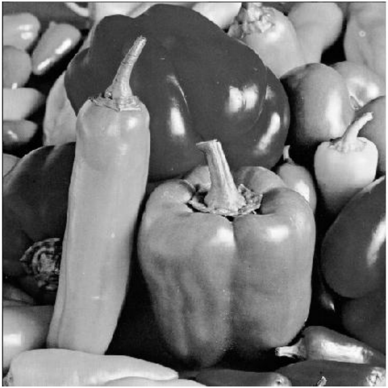

Introduction

1. Signal penalty regularization
   ROF model; Compressive sensing (CS); ...
   - l^2;
   - Total variation (TV), Total generalized variation (TGV) [1];
   - $l^0 \to l^1$, or $\|f\|_{l_q}^q := \sum_i |f_i|^q (0 < q < 1)$ [2];
   - $l^0 \to$ low rank matrix, like truncated norm l_{1-2}[3]: denoted as $l_{t,1-2}$ for sparse (vector) recovery and (matrix) rank minimization,

$$\|\mathbf{x}\|_{t,1-2} := \sum_{i \notin \Gamma_{\mathbf{x},t}} |x_i| - \sqrt{\sum_{i \notin \Gamma_{\mathbf{x},t}} x_i^2},$$

   for any $i \notin \Gamma_{\mathbf{x},t}$ and $j \in \Gamma_{\mathbf{x},t}$, $|x_i| \le |x_j|$.

2. Multi-penalty regularization

[1] Bredies K, Kunisch K, Pock T. *SIAM J. Imaging Sci.*, 2010.
[2] Chartrand R. *IEEE Signal Process. Lett.*, 2007.
[3] Ma T H, Lou Y F, Huang T Z. *SIAM J. Imaging Sci.*, 2017.

Outline

1. Introduction
2. The multi-penalty regularization modeling
3. The alternative iteration scheme
4. Convergence property of iteration process
5. Numerical experiments
6. Summary

Notation and Symbols

- **f**: image vector for an $N \times N$ two-dimensional image $f := (f_{m,n})$ where $m, n = 1, \cdots, N$.
- $\mathcal{F}$: Fourier transform.

Notation and Symbols

- **f**: image vector for an $N \times N$ two-dimensional image $f := (f_{m,n})$ where $m, n = 1, \cdots, N$.
- $\mathcal{F}$: Fourier transform.
- F: Fourier transform matrix, $F_{m,n} = e^{-i\frac{2\pi}{N}mn}$.
- **F**: Two-dimensional discrete Fourier transform (DFT) matrix,

$$\hat{\mathbf{f}} := \mathbf{vect}[F^T f F] = (F \otimes F)\mathbf{f} := \mathbf{F}\mathbf{f},$$

where $\otimes$ is the tensor product of two matrices.

Sampling matrix

P: the $N \times N$ matrix generating from the identity matrix $\mathcal{I}$ by setting its $N-M$ rows as null vectors, i.e.,

$$P = \mathrm{diag}(p_{11}, p_{22}, \cdots, p_{NN}), p_{ii} \in \{0, 1\}.$$

$P\hat{f}$: only take $M(\leq N)$ rows of $\hat{f}$,

$$\mathbf{vect}[P\hat{f}] = (\mathcal{I} \otimes P)\mathbf{vect}[\hat{f}] = (\mathcal{I} \otimes P)\hat{\mathbf{f}} := \mathbf{P}\hat{\mathbf{f}}.$$

Remark

$$\mathbf{vect}[P\hat{f}] = (\mathcal{I} \otimes P)\mathbf{vect}[\hat{f}] = (\mathcal{I} \otimes P)\hat{\mathbf{f}} := \mathbf{P}_r\hat{\mathbf{f}}.$$
$$\mathbf{vect}[\hat{f}P] = (P \otimes \mathcal{I})\mathbf{vect}[\hat{f}] = (P \otimes \mathcal{I})\hat{\mathbf{f}} := \mathbf{P}_c\hat{\mathbf{f}}.$$

Sampling operator

$\mathcal{P}_*$: random band sampling (RBS), i.e., takes both M_r-row sampling and M_c-column sampling together

$$\mathcal{P}_* : \hat{f} \to P_r \hat{f} + \hat{f} P_c - P_r \hat{f} \bigcap \hat{f} P_c.$$

R_{center}: the efficient elements among all the sampling elements,

$$R_{center} := \frac{m_r}{M_r} \times \frac{m_c}{M_c}.$$

R_{total}: the sampling ratio of $\mathcal{P}_*$,

$$R_{total} := \frac{N \times M_r + N \times M_c - M_r \times M_c}{N^2},$$

which m_r rows and m_c columns located in the center area.

General multi-penalty model

The reconstruction of f with the sparsity requirement under the basis $\{\psi_{m,n} : m, n = 1, \cdots, N\}$ can be modeled by

$$\begin{cases} \min_{\tilde{\mathbf{f}}}\{\|\tilde{\mathbf{f}}\|_{l^0} : \|\mathcal{P}\mathcal{F}\Psi[\tilde{\mathbf{f}}] - \mathcal{P}\hat{g}^\delta\|_F \leq \delta\}, \\ f := \Psi[\tilde{\mathbf{f}}], \end{cases} \tag{1}$$

$$J_\alpha(f) := \frac{1}{2}\|\mathcal{P}\mathcal{F}f - \mathcal{P}\hat{g}^\delta\|_F^2 + \alpha_1\|\Psi^{-1}[f]\|_{l^1} + \alpha_2|f|_{TV}. \tag{2}$$

With Charbonnier approximation, the model can be rewritten as

$$\min_f \left\{\frac{1}{2}\|\mathcal{P}\mathcal{F}f - \mathcal{P}\hat{g}^\delta\|_F^2 + \alpha_1\|\Psi^{-1}[f]\|_{l^1,\phi_\beta^C} + \alpha_2|f|_{TV,\phi_\beta^C}\right\}. \tag{3}$$

$\mathcal{P}\hat{g}^\delta$: the incomplete noisy frequency data;

α_1, α_2: regularizing parameters, $\alpha := (\alpha_1, \alpha_2) > 0$.

General multi-penalty model

Theorem 2.1

For given sampling operator $\mathcal{P}$ and $\alpha = \{\alpha_1, \alpha_2\} > 0, \beta \geq 0$, there exists a local minimizer $f^{*,\delta}_{\alpha,\beta}$ (maybe not unique) to the optimization problem (3) in $\mathbb{R}^{N\times N}$. Moreover, $f^{*,\delta}_{\alpha,\beta}$ has the following error estimates:

$$\begin{cases} \|\mathcal{P}\mathcal{F}f^{*,\delta}_{\alpha,\beta} - \mathcal{P}\hat{g}^\delta\|_F^2 \leq \delta^2 + 2(\alpha_1+\alpha_2)N^2\sqrt{\beta} \\ \qquad\qquad + 2\alpha_1\|\Psi^{-1}[f^\dagger]\|_{l^1} + 2\alpha_2|f^\dagger|_{TV}, \\ \|\Psi^{-1}[f^{*,\delta}_{\alpha,\beta}]\|_{l^1} \leq \frac{\delta^2}{2\alpha_1} + \frac{\alpha_2}{\alpha_1}|f^\dagger|_{TV} + (1+\frac{\alpha_2}{\alpha_1})N^2\sqrt{\beta} \\ \qquad\qquad + \|\Psi^{-1}[f^\dagger]\|_{l^1}, \\ |f^{*,\delta}_{\alpha,\beta}|_{TV} \leq \frac{\delta^2}{2\alpha_2} + \frac{\alpha_1}{\alpha_2}\|\Psi^{-1}[f^\dagger]\|_{l^1} + (1+\frac{\alpha_1}{\alpha_2})N^2\sqrt{\beta} + |f^\dagger|_{TV} \end{cases} \tag{4}$$

where $f^\dagger \in \mathbb{R}^{N\times N}$ is the grey matrix for exact image.

· Liu X M, Liu J J. On image restoration from random sampling noisy frequency data with regularization. *Inverse Problems in Science and Engineering*, 2018.

General multi-penalty model

(4a) the data-fitting error: when $\alpha_1 = \alpha_2 = \delta^2$ and small constant $\beta > 0$, the optimal order is $O(\delta^2)$;

(4b) the sparsity estimate: depends on the ratio $\frac{\alpha_2}{\alpha_1}$;

(4c) the smoothness estimate: depends on the ratio $\frac{\alpha_1}{\alpha_2}$.

We can take $\alpha_1 = \delta, \alpha_2 = \delta^2, \beta = \delta^2$ such that

$$\|\mathcal{P}\mathcal{F}f^{*,\delta}_{\alpha,\beta} - \mathcal{P}\hat{g}^{\delta}\|^2_F \le C\delta^2,$$

$$0 \le \|\Psi^{-1} \circ f^{*,\delta}_{\alpha,\beta}\|_{l^1} - \|\Psi^{-1} \circ f^{\dagger}\|_{l^1} \le C\delta,$$

$$0 \le |f^{*,\delta}_{\alpha,\beta}|_{TV} - |f^{\dagger}|_{TV} \le C\frac{1}{\delta}.$$

Simplify multi-penalty model

$$\min_{f}\left\{\frac{1}{2}\|\mathcal{P}\mathcal{F}f-\mathcal{P}\hat{g}^{\delta}\|_F^2+\alpha_1\|\Psi^{-1}[f]\|_{l^1}+\alpha_2|f|_{TV}\right\} \tag{2}$$

Difficulties:

1) l^1 penalty term: with complex sparsity framework.
2) huge computational works.
3) non-smooth, non-convex.

Simplify multi-penalty model

$$\min_f \left\{ \frac{1}{2} \|\mathcal{P}\mathcal{F}f - \mathcal{P}\hat{g}^\delta\|_F^2 + \alpha_1 \|\Psi^{-1}[f]\|_{l^1} + \alpha_2 |f|_{TV} \right\} \qquad (2)$$

Difficulties:

1) l^1 penalty term: with complex sparsity framework.
2) huge computational works.
3) non-smooth, non-convex.

The sparse basis Ψ (like Danbechies) $\Rightarrow$ boundary operator

$$C_1 \|\mathbf{vect}[f]\|_{l^1} \leq \|\Psi^{-1}[f]\|_{l^1} \leq C_2 \|\mathbf{vect}[f]\|_{l^1}.$$

$$(2) \Rightarrow \min_f \left\{ \frac{1}{2} \|\mathcal{P}\mathcal{F}f - \mathcal{P}\hat{g}^\delta\|_F^2 + \alpha_1 \|\mathbf{vect}[f]\|_{l^1} + \alpha_2 |f|_{TV} \right\} \qquad (5)$$

Outline

1. Introduction
2. The multi-penalty regularization modeling
3. The alternative iteration scheme
4. Convergence property of iteration process
5. Numerical experiments
6. Summary

Outline

1. Introduction
2. The multi-penalty regularization modeling
3. The alternative iteration scheme
   - Reformulation of the simplify model
   - Fast algorithm based on alternative iteration
4. Convergence property of iteration process
5. Numerical experiments
6. Summary

Simplify model

$$J^{Z}_{\alpha,\nu}(f) := \frac{1}{2}\left\|\mathcal{P}\mathcal{F}f - \mathcal{P}\hat{g}^{\delta}\right\|_{F}^{2} + \alpha_1\|\mathbf{vect}[f]\|_{l^1,\phi^{Z}_{\nu}} + \alpha_2|f|_{TV} \tag{6}$$

for $(Z,\nu) = (C,\beta)$ or $(Z,\nu) = (H,\epsilon)$.

$$\|\mathbf{vect}[f]\|_{l^1,\phi^{C}_{\beta}} = \sum_{m,n=1}^{N} \phi^{C}_{\beta}\left(f_{m,n}\right), \quad \|\mathbf{vect}[f]\|_{l^1,\phi^{H}_{\epsilon}} = \sum_{m,n=1}^{N} \phi^{H}_{\epsilon}\left(f_{m,n}\right).$$

$$\phi^{C}_{\beta}(s) := \sqrt{s^2+\beta}, \qquad \phi^{H}_{\epsilon}(s) := \begin{cases} \frac{s^2}{2\epsilon}, & |s| \le \epsilon, \\ |s| - \frac{\epsilon}{2}, & |s| > \epsilon. \end{cases}$$

Simplify model

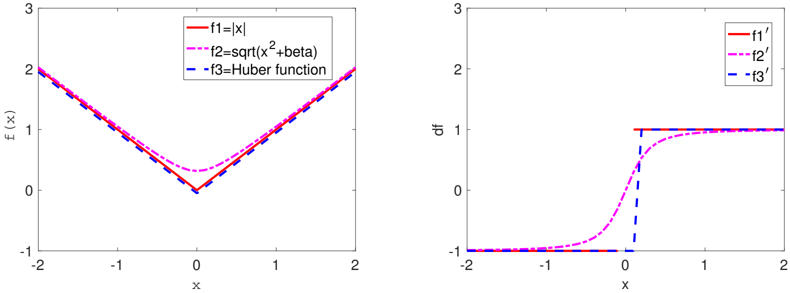

(a) Three functions (b) The derivatives of three functions

Figure 2: The absolute value function comparing with Charbonnier and Huber function, $\beta = \epsilon = 0.1$.

Simplify model

Model (6) can be rewritten as

$$\min_{\mathbf{f}} \left\{ J^{Z}_{\alpha,\nu}(\mathbf{f}) := \frac{1}{2} \left\| \mathbf{PFf} - \mathbf{P}\hat{\mathbf{g}}^{\delta} \right\|^2_{l^2} + \alpha_1 \|\mathbf{f}\|_{l^1,\phi^Z_\nu} + \alpha_2 |\mathbf{f}|_{TV} \right\}, \tag{7}$$

$$|\mathbf{f}|_{TV} = \sum_{j=1}^{N^2} \|((\nabla^{x_1}\mathbf{f})_j, (\nabla^{x_2}\mathbf{f})_j)\|_{l^2}, \tag{8}$$

$$\|\mathbf{f}\|_{l^1,\phi^C_\beta} = \sum_{j=1}^{N^2} \phi^C_\beta(\mathbf{f}_j), \quad \|\mathbf{f}\|_{l^1,\phi^H_\epsilon} = \sum_{j=1}^{N^2} \phi^H_\epsilon(\mathbf{f}_j), \tag{9}$$

where $j := j(m,n) = (n-1) \times N + m$ for $m, n = 1, \cdots, N$.

Simplify model

$$(\nabla^{x_1}\mathbf{f})_j := ((I \otimes D_-)\mathbf{f})_j,\ (\nabla^{x_2}\mathbf{f})_j := ((D_- \otimes I)\mathbf{f})_j, \qquad (10)$$

where $I \otimes D_-, D_- \otimes I \in \mathbb{R}^{N^2 \times N^2}$ are block-circulant-circulant-block (BCCB) matrices with tensor product $\otimes$, $j = 1, \cdots, N^2$.

$$\begin{aligned} D_- &= \begin{pmatrix} -1 & 1 & 0 & \cdots & 0 & 0 & 0 \\ 0 & -1 & 1 & \cdots & 0 & 0 & 0 \\ \cdots & \cdots & \cdots & \cdots & \cdots & \cdots & \cdots \\ 0 & 0 & 0 & \cdots & -1 & 1 & 0 \\ 0 & 0 & 0 & \cdots & 0 & -1 & 1 \\ 1 & 0 & 0 & \cdots & 0 & 0 & -1 \end{pmatrix}_{N \times N} \\ : &= \mathbf{circulant}(-1, 0, \cdots, 0, 1). \end{aligned}$$

Outline

1 Introduction

2 The multi-penalty regularization modeling

3 The alternative iteration scheme
- Reformulation of the simplify model
- Fast algorithm based on alternative iteration

4 Convergence property of iteration process

5 Numerical experiments

6 Summary

Alternative iteration scheme

Let $\mathbf{w} = (\mathbf{w}_1, \cdots, \mathbf{w}_{N^2}) \in \mathbb{R}^{2\times N^2}$ with each component $\mathbf{w}_j = (\mathbf{w}_j^1, \mathbf{w}_j^2)^T \in \mathbb{R}^{2\times 1}$. We rewrite the unconstrained optimization problem (7) as the following constrained one

$$\begin{cases} \min\limits_{\mathbf{w},\mathbf{f}} & \widetilde{J}^Z_{\alpha,\nu}(\mathbf{w},\mathbf{f}) \\ \text{s.t.} & \mathbf{w}_j - (\nabla \mathbf{f})_j = (0,0)^T, \quad j = 1,\cdots,N^2 \end{cases} \tag{11}$$

with the cost functional defined by

$$\widetilde{J}^Z_{\alpha,\nu}(\mathbf{w},\mathbf{f}) := \frac{1}{2}\left\|\mathbf{PFf} - \mathbf{P}\hat{\mathbf{g}}^\delta\right\|^2_{l^2} + \alpha_1 \|\mathbf{f}\|_{l^1,\phi^Z_\nu} + \alpha_2 \sum_{j=1}^{N^2} \|\mathbf{w}_j\|_{l^2}. \tag{12}$$

Alternative iteration scheme

$$\begin{cases} \min\limits_{\mathbf{w}} & \sum\limits_{j=1}^{N^2} \|\mathbf{w}_j\|_{l^2} \\ \text{s.t.} & \mathbf{w}_j - (\nabla \mathbf{f}^{(k)})_j = (0,0)^T, \quad j = 1,\cdots,N^2 \end{cases} \tag{13}$$

$$\begin{aligned} \mathcal{L}^{\boldsymbol{\lambda}}(\mathbf{w}) &= \sum_{j=1}^{N^2} \|\mathbf{w}_j\|_{l^2} - \\ & (\boldsymbol{\lambda}_1^T, \cdots, \boldsymbol{\lambda}_{N^2}^T) \left((\mathbf{w}_1 - \nabla \mathbf{f}_1^{(k)})^T, \cdots, (\mathbf{w}_{N^2} - \nabla \mathbf{f}_{N^2}^{(k)})^T \right)^T \end{aligned}$$

with the Lagrange multiplier $\boldsymbol{\lambda} := (\boldsymbol{\lambda}_1, \cdots, \boldsymbol{\lambda}_{N^2}) \in \mathbb{R}^{2\times N^2}$.

Alternative iteration scheme

$$
\begin{aligned}
\mathcal{L}^{\boldsymbol{\lambda},\tau}(\mathbf{w}) : &= \mathcal{L}^{\boldsymbol{\lambda}}(\mathbf{w}) + \frac{\tau}{2}\left\|\left((\mathbf{w}_1 - \nabla \mathbf{f}_1^{(k)}), \cdots, (\mathbf{w}_{N^2} - \nabla \mathbf{f}_{N^2}^{(k)})\right)\right\|_{l^2}^2 \\
&\equiv \sum_{j=1}^{N^2}\left(\|\mathbf{w}_j\|_{l^2} - \boldsymbol{\lambda}_j^T(\mathbf{w}_j - \nabla \mathbf{f}_j^{(k)}) + \frac{\tau}{2}\left\|\mathbf{w}_j - \nabla \mathbf{f}_j^{(k)}\right\|_{l^2}^2\right) \\
&\equiv \sum_{j=1}^{N^2}\left(\|\mathbf{w}_j\|_{l^2} + \frac{\tau}{2}\left\|\mathbf{w}_j - \nabla \mathbf{f}_j^{(k)} - \frac{1}{\tau}\boldsymbol{\lambda}_j\right\|_{l^2}^2 - \frac{1}{2\tau}\|\boldsymbol{\lambda}_j\|_{l^2}^2\right) \quad (14)
\end{aligned}
$$

with some weight $\tau > 0$.

Alternative iteration scheme

$$\min_{\mathbf{w}} \widetilde{J}_{\alpha,\nu}^{Z,\boldsymbol{\lambda},\tau}(\mathbf{w}, \mathbf{f}^{(k)}), \tag{15}$$

where the cost functional is defined as

$$\begin{aligned}\widetilde{J}_{\alpha,\nu}^{Z,\boldsymbol{\lambda},\tau}(\mathbf{w}, \mathbf{f}^{(k)}) &= \frac{1}{2}\left\|\mathbf{PFf}^{(k)} - \mathbf{P}\hat{\mathbf{g}}^{\delta}\right\|_{l^2}^2 + \alpha_1 \|\mathbf{f}^{(k)}\|_{l^1,\phi_\nu^Z} + \\ & \alpha_2 \sum_{j=1}^{N^2} \left(\|\mathbf{w}_j\|_{l^2} + \frac{\tau}{2}\left\|\mathbf{w}_j - \nabla \mathbf{f}_j^{(k)} - \frac{1}{\tau}\boldsymbol{\lambda}_j\right\|_{l^2}^2 - \frac{1}{2\tau}\|\boldsymbol{\lambda}_j\|_{l^2}^2 \right).\end{aligned} \tag{16}$$

Multi-regularizing parameters: $\alpha_1, \alpha_2 > 0$;
Multiplier parameter: $\boldsymbol{\lambda} \in \mathbb{R}^{2\times N^2}$;
Penalty factor: $\tau > 0$.

Inner iteration

In generating the minimizer $\mathbf{w}^{(k+1)}$ from (15) by inner iteration, i.e.,

Step 1: fixed $\mathbf{f}$

The Euler equation for $\widetilde{J}_{\alpha,\nu}^{Z,\boldsymbol{\lambda}^{(k),l},\tau}(\mathbf{w},\mathbf{f}^{(k)})$ with respect to $\mathbf{w}$:

$$\frac{\mathbf{w}_j}{\|\mathbf{w}_j\|_{l^2}} + \tau(\mathbf{w}_j - \mathbf{t}_j^{(k),l}) = \mathbf{0}, \quad j = 1, \cdots, N^2 \tag{17}$$

with $\mathbf{t}_j^{(k),l} := \nabla \mathbf{f}_j^{(k)} + \boldsymbol{\lambda}_j^{(k),l}/\tau \in \mathbb{R}^{2\times 1}$. The solution to (17) is

$$\mathbf{w}_j^{(k),l+1} = \max\left\{1 - \frac{1}{\tau}\frac{1}{\left\|\mathbf{t}_j^{(k),l}\right\|_{l^2}}, 0\right\}\mathbf{t}_j^{(k),l}. \tag{18}$$

Inner iteration

To update the Lagrange multiplier $\boldsymbol{\lambda}^{(k),l}$ for the inner iteration by

$$\begin{aligned} \boldsymbol{\lambda}_j^{(k),l+1} : &= \boldsymbol{\lambda}_j^{(k),l} - \tau(\mathbf{w}_j^{(k),l+1} - \nabla \mathbf{f}_j^{(k)}) \\ &= \begin{cases} \dfrac{\mathbf{w}_j^{(k),l+1}}{\left\| \mathbf{w}_j^{(k),l+1} \right\|_{l^2}}, & \mathbf{w}_j^{(k),l+1} \neq \mathbf{0}, \\ \boldsymbol{\lambda}_j^{(k),l} + \tau \nabla \mathbf{f}_j^{(k)}, & \mathbf{w}_j^{(k),l+1} = \mathbf{0}. \end{cases} \end{aligned} \tag{19}$$

Remark

$\mathbf{w}_j^{(k),l+1} = \mathbf{0}$ means $\left\| \mathbf{t}_j^{(k),l} \right\|_{l^2} \leq \frac{1}{\tau}$, i.e., we always have $\left\| \boldsymbol{\lambda}_j^{(k),l+1} \right\| \leq 1$ for all $l = 1, \cdots$ at any fixed k and $j = 1, \cdots, N^2$.

Inner iteration

The inner iteration will be stopped, if

$$\left\| \mathbf{w}^{(k),l+1} - \nabla \mathbf{f}^{(k)} \right\|_{l^2} \leq \varepsilon_{tol} \tag{20}$$

at some step $l = L(k)$ for specified small tolerance $\varepsilon_{tol} > 0$.

Then the main loop is going on with

$$\mathbf{w}^{(k+1)} := \mathbf{w}^{(k),L(k)+1}, \quad \boldsymbol{\lambda}^{(k+1)} := \boldsymbol{\lambda}^{(k),L(k)+1}. \tag{21}$$

Main loop

Step 2: for fixed $\mathbf{w}$ and λ

$$D_+ := -D_-^T. \tag{22}$$

The Euler equation for the cost functional $\widetilde{J}_{\alpha,\nu}^{Z,\boldsymbol{\lambda}^{(k+1)},\tau}(\mathbf{w}^{(k+1)},\mathbf{f})$:

$$\overline{\mathbf{F}}^T\mathbf{P}^T(\mathbf{PFf}-\mathbf{P}\hat{\mathbf{g}}^\delta)-\alpha_2(I\otimes D_+,D_+\otimes I)\vec{\boldsymbol{\lambda}}^{(k+1)}+$$
$$\alpha_2\tau\,(I\otimes D_+,D_+\otimes I)\left[\vec{\mathbf{w}}^{(k+1)}-\begin{pmatrix} I\otimes D_- \\ D_-\otimes I\end{pmatrix}\mathbf{f}\right]+\alpha_1\Lambda^Z[\mathbf{f}]\mathbf{f}=\mathbf{0}. \tag{23}$$

$$\Lambda^Z[\mathbf{f}] := \mathrm{diag}(a_1^Z[\mathbf{f}],a_2^Z[\mathbf{f}],\cdots,a_{N^2}^Z[\mathbf{f}]),$$

$$a_l^C[\mathbf{f}] := \frac{1}{\sqrt{|\mathbf{f}_l|^2+\beta}},\qquad a_l^H[\mathbf{f}] := \begin{cases} 1/\epsilon, & |\mathbf{f}_l|\le\epsilon,\\ \mathrm{sgn}(\mathbf{f}_l)/\mathbf{f}_l, & |\mathbf{f}_l|>\epsilon.\end{cases}$$

Nonlinear!

Main loop

By linearizing the last nonlinear term $\Lambda^Z[\mathbf{f}]\mathbf{f}$ of (23) in the way

$$\Lambda^Z[\mathbf{f}]\mathbf{f} \approx A^Z_{(k)}\mathbf{f} + \Lambda^Z[\mathbf{f}^{(k)}]\mathbf{f}^{(k)} - A^Z_{(k)}\mathbf{f}^{(k)},$$

where

$$A^Z_{(k)} := \max\{a^Z_j[\mathbf{f}^{(k)}] : \ j = 1, \cdots, N^2\}.$$

Nonlinear $\Rightarrow$ linear!

$$\mathbf{L}^{(k)}\mathbf{f}^{(k+1)} = \mathbf{b}^{(k)}, \tag{24}$$

$$\begin{cases} \mathbf{L}^{(k)} = -\alpha_2\tau\,(I\otimes D_+, D_+\otimes I)\begin{pmatrix} I\otimes D_- \\ D_-\otimes I\end{pmatrix} + \alpha_1 A^Z_{(k)}\mathbf{I} + \overline{\mathbf{F}}^T\mathbf{P}^T\mathbf{P}\mathbf{F}, \\ \mathbf{b}^{(k)} = \alpha_2\,(I\otimes D_+, D_+\otimes I)\left(-\tau\vec{\mathbf{w}}^{(k+1)} + \vec{\boldsymbol{\lambda}}^{(k+1)}\right) + \overline{\mathbf{F}}^T\mathbf{P}^T\mathbf{P}\hat{\mathbf{g}}^\delta + \\ \qquad \alpha_1(A^Z_{(k)}\mathbf{I} - \Lambda^Z[\mathbf{f}^{(k)}])\mathbf{f}^{(k)}. \end{cases}$$

Main loop

Applying two-dimensional DFT $\mathcal{F}$ on both sides of (24), we obtain

$$\widetilde{\mathbf{L}}^{(k)}\hat{\mathbf{f}}^{(k+1)} = \hat{\mathbf{b}}^{(k)}, \tag{25}$$

where $\hat{\mathbf{f}}^{(k+1)} = \mathcal{F}[\mathbf{f}^{(k+1)}] = \mathbf{F}\mathbf{f}^{(k+1)}$ and

$$\begin{cases} \widetilde{\mathbf{L}}^{(k)} = \mathbf{F}\mathbf{L}^{(k)}\mathbf{F}^{-1} \\ \qquad = -\alpha_2\tau\mathbf{F}\left(\mathbb{D}_1 + \mathbb{D}_2\right)\mathbf{F}^{-1} + \alpha_1 A^Z_{(k)}\mathbf{I} + \mathbf{P}^T\mathbf{P}, \\ \hat{\mathbf{b}}^{(k)} = \mathbf{F}\left[\alpha_2(I\otimes D_+, D_+\otimes I)\left(-\tau\vec{\mathbf{w}}^{(k+1)} + \vec{\boldsymbol{\lambda}}^{(k+1)}\right)\right] + \mathbf{P}^T\mathbf{P}\hat{\mathbf{g}}^\delta + \\ \qquad \alpha_1\mathbf{F}(A^Z_{(k)}\mathbf{I} - \Lambda^Z[\mathbf{f}^{(k)}])\mathbf{f}^{(k)}. \end{cases}$$

Main loop

$\mathbb{D}_i (i = 1, 2)$ are the $N^2 \times N^2$ block-circulate-circulate-block (BCCB) matrices generated by

$$\mathbb{D}_1 := \mathbf{bccb} \circ D_*, \quad \mathbb{D}_2 := \mathbf{bccb} \circ D_*^T.$$

$D_* = (\mathbf{d}_*, \mathbf{0}, \cdots, \mathbf{0})$: $N \times N$ matrix.

$$\mathbf{d}_* = (-2, 2)^T \text{ for } N = 2;$$
$$\mathbf{d}_* = (-2, 1, \underbrace{0, \cdots, 0}_{N-3}, 1)^T \text{ for } N = 3, 4, \cdots.$$

Main loop

$$\mathbf{F}\left(\mathbb{D}_1+\mathbb{D}_2\right)=-\left(\mathbb{L}_1+\mathbb{L}_2\right)\mathbf{F}.$$

$\mathbb{L}_i(i=1,2)$: diagonal matrix, i.e., $\mathbb{L}_1+\mathbb{L}_2=\mathrm{diag}(\mathbf{vec}[\mathbb{L}])$.

$$\mathrm{l}_{m,n}=4-2\left(\cos\frac{2\pi}{N}(m-1)+\cos\frac{2\pi}{N}(n-1)\right),\quad m,n=1,\cdots,N.$$

$$\widetilde{\mathbf{L}}^{(k)}=\alpha_2\tau\left(\mathbb{L}_1+\mathbb{L}_2\right)+\alpha_1 A^Z_{(k)}\mathbf{I}+\mathbf{P}^T\mathbf{P}. \tag{26}$$

Remark

$\mathbb{L}_i(i=1,2)$ are diagonal matrix, with the elements being the negative eigenvalues of $\mathbb{D}_i$ (Prop. 5.31 in [5]).

[5] Vogel C R. Computational Methods for Inverse Problems, SIAM, 2002.

Main loop

The stopping rules could be one of the inequalities

$$\text{either } \left\|\mathbf{P}\hat{\mathbf{f}}^{(k+1)} - \mathbf{P}\hat{\mathbf{g}}^{\delta}\right\|_{l^2} \leq \delta \text{ or } k \leq K_0. \tag{27}$$

δ: the noise level;

K_0: the maximum main iterative step number.

Remark

$$\mathbf{f}_j^{(k+1)} = \begin{cases} \mathbf{f}_j^{(k+1)}, & 0 \leq \mathbf{f}_j^{(k+1)} \leq 1 \\ 0, & \mathbf{f}_j^{(k+1)} < 0 \\ 1, & \mathbf{f}_j^{(k+1)} > 1. \end{cases} \tag{28}$$

The alternative iteration scheme (AIS)

Algorithm Alternative iteration scheme (AIS)

Input: noisy frequency data $\{\hat{g}^{\delta}_{m',n'} : m', n' = 1, \cdots, N\}$, sampling matrix $\mathbf{P} \in \mathbb{R}^{N^2 \times N^2}$, parameters $\alpha_1, \alpha_2, \beta, \epsilon, \tau, K_0$, tolerance ε_{tol}

Set initial value $\mathbf{f}^{(0)} = \mathbf{0} \in \mathbb{R}^{N^2 \times 1}, \boldsymbol{\lambda}^{(0)} = \mathbf{0} \in \mathbb{R}^{2 \times N^2}$

Do exterior loop from $k = 1, 2, \cdots$

while $\left\|\mathbf{PFf}^{(k)} - \mathbf{P}\hat{\mathbf{g}}^{\delta}\right\|_{l^2} > \delta$ or $k < K_0$ **do**

  Do inner loop from $l = 0, 1, \ldots$ with $\boldsymbol{\lambda}^{(k),0} = \boldsymbol{\lambda}^{(k-1)} \in \mathbb{R}^{2 \times N^2}$

  while $\left\|\mathbf{w}^{(k),l+1} - \nabla\mathbf{f}^{(k)}\right\|_{l^2} > \varepsilon_{tol}$ or $l < L_0$ **do**

    Determine $\mathbf{w}_j^{(k),l+1}$ by (18) for all j

    Update $\boldsymbol{\lambda}_j^{(k),l+1} \leftarrow \boldsymbol{\lambda}_j^{(k),l} - \tau(\mathbf{w}_j^{(k),l+1} - \nabla\mathbf{f}_j^{(k)})$ by (19) for all j

  end while

  Update $\mathbf{w}^{(k+1)} \leftarrow \mathbf{w}^{(k),l+1}$, $\boldsymbol{\lambda}^{(k+1)} \leftarrow \boldsymbol{\lambda}^{(k),l+1}$

  Determine $\mathbf{f}^{(k+1)}$ by solving (25) and then taking IFFT

end while

Modify $\mathbf{f}^{(k+1)}$ by (28)

Output: $f^{(k+1)} \in \mathbb{R}^{N \times N} \leftarrow \mathbf{f}^{(k+1)} \in \mathbb{R}^{N^2 \times 1}$

Outline

1. Introduction
2. The multi-penalty regularization modeling
3. The alternative iteration scheme
4. Convergence property of iteration process
5. Numerical experiments
6. Summary

Theorem

Theorem 4.1

For any fixed $\alpha_1, \alpha_2 > 0$, *if we take* $\tau > 0$ *small and* $\beta > 0$ *large appropriately, the iterative sequences* $\{\mathbf{f}^{(k)} : k \in \mathbb{N}\}$ *from the proposed AIS almost converges for small tolerance* $\varepsilon_{tol} > 0$.

Remark

In the following proof, we consider the model (7) mainly (Charbonnier approximation, called C-SMRM), all the notations and analysis are also applicable to Huber approximation H-SMRM.

Proof

- C-SMRM with $\phi_\beta^C(s)$:

$$\left\|\boldsymbol{\lambda}_j^{(k),l+1}\right\|_{l^2} \le 1 \Rightarrow \exists \text{ subsequence } \left\{\boldsymbol{\lambda}_j^{(k),l} : \; l \in \mathbb{N}\right\}, \text{ s.t. } \boldsymbol{\lambda}_j^{(k),l} \overset{l\to\infty}{\longrightarrow} \boldsymbol{\lambda}_j^{(k),*}$$

$$\Rightarrow \; \tau\left(\mathbf{w}_j^{(k),l+1} - \nabla \mathbf{f}_j^{(k)}\right) \overset{l\to\infty}{\longrightarrow} 0 \; \Rightarrow \; \mathbf{w}_j^{(k),l+1} - \nabla \mathbf{f}_j^{(k)} \overset{l\to\infty}{\longrightarrow} 0.$$

$$\begin{aligned}
&\left(\alpha_2\tau\left(\mathbb{L}_1+\mathbb{L}_2\right)+\alpha_1 A_{(k)}^C \mathbf{I}+\mathbf{P}^T\mathbf{P}\right)\left(\hat{\mathbf{f}}^{(k+1)}-\hat{\mathbf{f}}^{(k)}\right) \\
= \; &\alpha_2\tau(\mathbb{L}_1+\mathbb{L}_2)(\hat{\mathbf{f}}^{(k)}-\hat{\mathbf{f}}^{(k-1)}) - \alpha_2\tau\varepsilon_{tol}\mathbf{F}(\tilde{q}_k-\tilde{q}_{k-1}) + \\
&\alpha_2\mathbf{F}(I\otimes D_+, D_+\otimes I)(\vec{\boldsymbol{\lambda}}^{(k+1)}-\vec{\boldsymbol{\lambda}}^{(k)}) + \\
&\alpha_1\mathbf{F}(A_{(k-1)}^C\mathbf{I}-\Lambda^C[\mathbf{f}^{(k)}])(\mathbf{f}^{(k)}-\mathbf{f}^{(k-1)}) + \\
&\alpha_1\mathbf{F}(\Lambda^C[\mathbf{f}^{(k-1)}]-\Lambda^C[\mathbf{f}^{(k)}])\mathbf{f}^{(k-1)}.
\end{aligned} \tag{29}$$

q_k: satisfied $\mathbf{w}^{(k+1)} = \nabla\mathbf{f}^{(k)} + q_k\varepsilon_{tol}$, $\|\tilde{q}_k\| = \|q_k\| \le 1.$

Proof

1) The updating process $\boldsymbol{\lambda}_j^{(k+1)} := \boldsymbol{\lambda}_j^{(k)} - \tau(\mathbf{w}_j^{(k+1)} - \nabla \mathbf{f}_j^{(k)})$:

$$\begin{aligned} \vec{\boldsymbol{\lambda}}^{(k+1)} - \vec{\boldsymbol{\lambda}}^{(k)} &= \mathbf{vect}[(\boldsymbol{\lambda}^{(k+1)} - \boldsymbol{\lambda}^{(k)})^T] \\ &= -\tau \mathbf{vect}[(\mathbf{w}^{(k+1)} - \nabla \mathbf{f}^{(k)})^T], \end{aligned}$$

$$\left\| \vec{\boldsymbol{\lambda}}^{(k+1)} - \vec{\boldsymbol{\lambda}}^{(k)} \right\| \leq \tau \varepsilon_{tol}.$$

2) From the expression of $\Lambda^C[\mathbf{f}]$ and $\left\|\mathbf{f}^{(k)}\right\|, \left\|\mathbf{f}^{(k-1)}\right\| \leq 1$:

$$\left\| A^C_{(k-1)} \mathbf{I} - \Lambda^C[\mathbf{f}^{(k)}] \right\| \leq \frac{1}{\sqrt{\beta^3}} \left\| \mathbf{f}^k - \mathbf{f}^{k-1} \right\|,$$

$$\left\| \Lambda^C[\mathbf{f}^{(k-1)}] - \Lambda^C[\mathbf{f}^{(k)}] \right\| \leq \frac{1}{\sqrt{\beta^3}} \left\| \mathbf{f}^k - \mathbf{f}^{k-1} \right\|.$$

Proof

3) For some $l_{j0} \neq 0$:

$$\max_{j=1,\cdots,N^2} \frac{\alpha_2 \tau l_j}{\alpha_2 \tau l_j + \alpha_1 A^C_{(k)} + p_j} = \frac{\alpha_2 \tau l_{j0}}{\alpha_2 \tau l_{j0} + \alpha_1 A^C_{(k)} + p_{j0}} \leq \frac{8\alpha_2 \tau}{\alpha_1 A^C_{(k)}},$$

$$\begin{aligned} & \left\| \left(\alpha_2 \tau \left(\mathbb{L}_1 + \mathbb{L}_2 \right) + \alpha_1 A^C_{(k)} \mathbf{I} + \mathbf{P}^T \mathbf{P} \right)^{-1} \right\|_\infty \\ = & \max_{j=1,\cdots,N^2} \frac{1}{\alpha_2 \tau l_j + \alpha_1 A^C_{(k)} + p_j} \leq \frac{1}{\alpha_1 A^C_{(k)}}. \end{aligned}$$

l_j, p_j: the diagonal elements, $0 \leq l_j \leq 8$, $p_j = 0, 1$;

4) $A^C_{(k)}$: $\frac{1}{\sqrt{1+\beta}} \leq A^C_{(k)} \leq \frac{1}{\sqrt{\beta}}$.

Proof

$$1)-4) \Rightarrow \left\|\mathbf{f}^{(k+1)}-\mathbf{f}^{(k)}\right\|$$

$$\le \frac{8\alpha_2\tau+\alpha_1\frac{C}{\sqrt{\beta^3}}}{\alpha_1 A_{(k)}^C}\left\|\mathbf{f}^{(k)}-\mathbf{f}^{(k-1)}\right\|+\frac{C}{\alpha_1 A_{(k)}^C}\alpha_2\tau\varepsilon_{tol}$$

$$\le \underbrace{\frac{\sqrt{1+\beta}}{\alpha_1}\left(8\alpha_2\tau+\frac{C\alpha_1}{\sqrt{\beta^3}}\right)}_{q_1\in(0,1)}\left\|\mathbf{f}^{(k)}-\mathbf{f}^{(k-1)}\right\|+\underbrace{\frac{C\sqrt{1+\beta}}{\alpha_1}\alpha_2\tau}_{q_2\in(0,1)}\varepsilon_{tol},$$

$$\left\|\mathbf{f}^{(k+1)}-\mathbf{f}^{(k)}\right\| \le q_1^k\left\|\mathbf{f}^{(1)}-\mathbf{f}^{(0)}\right\|+\frac{1}{1-q_1}\varepsilon_{tol}.$$

almost converges: $\varepsilon_{tol}>0$!

Proof

- H-SMRM with $\phi_\epsilon^H(s)$:

2) $\left\| A^H_{(k-1)}\mathbf{I} - \Lambda^H[\mathbf{f}^{(k)}] \right\| < \frac{1}{\epsilon}, \quad \left\| \Lambda^H[\mathbf{f}^{(k-1)}] - \Lambda^H[\mathbf{f}^{(k)}] \right\| < \frac{1}{\epsilon}.$

3) $\left\| \left(\alpha_2 \tau (\mathbb{L}_1 + \mathbb{L}_2) + \alpha_1 A^H_{(k)}\mathbf{I} + \mathbf{P}^T\mathbf{P} \right)^{-1} \right\|_\infty \leq \frac{1}{\alpha_1 A^H_{(k)}}.$

4) $1 \leq A^H_{(k)} \leq \frac{1}{\epsilon}.$

$$1) - 4) \quad \Rightarrow \quad \left\| \mathbf{f}^{(k+1)} - \mathbf{f}^{(k)} \right\| \leq \underbrace{\frac{1}{\alpha_1}\left(8\alpha_2\tau + \alpha_1 \frac{C}{\epsilon} \right)}_{q_1 \in (0,1)} \left\| \mathbf{f}^{(k)} - \mathbf{f}^{(k-1)} \right\| + \underbrace{\frac{C}{\alpha_1}\alpha_2\tau\, \varepsilon_{tol}}_{q_2 \in (0,1)}. \quad \square$$

Theorem

Theorem 4.2

If $\{\mathbf{f}^{(k)} : k \in \mathbb{N}\}$ *and* $\{\mathbf{f}_E^{(k)} : k \in \mathbb{N}\}$ *are generated from the same initial guess* $\mathbf{f}^{(0)}$, *then for small* $\alpha_2, \tau, \varepsilon_{tol} > 0$ *and large* $\alpha_1, \beta > 0$, *it follows*

$$\lim_{k\to\infty} \left\| \mathbf{f}^{(k)} - \mathbf{f}_E^{(k)} \right\| \approx 0 \tag{30}$$

up to the accuracy $O(\alpha_2 + \tau\varepsilon_{tol})$, *where* $\lim_{k\to\infty} \mathbf{f}^{(k)}$ *is the minimizer of the cost functional* $\lim_{k\to\infty} \widetilde{J}_{\alpha,\beta}^{C,\boldsymbol{\lambda}^{(k)},\tau}(\nabla\mathbf{f}, \mathbf{f})$ *related to* $\mathbf{f}^{(0)}, \boldsymbol{\lambda}^{(0)}$.

Proof

Define $\mathbf{z}^{(k+1)} := \mathbf{f}^{(k+1)} - \mathbf{f}_E^{(k+1)}$. It follows from direct computations that $\mathbf{f}^{(k)} - \mathbf{f}_E^{(k)}$ with Fourier transform meets

$$
\begin{aligned}
& \left(\mathbf{P}^T\mathbf{P} + \alpha_2\tau(\mathbb{L}_1 + \mathbb{L}_2) + \alpha_1 \mathbf{F}\Lambda^C[\mathbf{f}_E^{(k+1)}]\overline{\mathbf{F}}^T\right)(\hat{\mathbf{z}}^{(k+1)} - \hat{\mathbf{z}}^{(k)}) \\
= \ & \alpha_2 \mathbf{F}(I \otimes D_+, D_+ \otimes I)((\vec{\boldsymbol{\lambda}}^{(k+1)} - \vec{\boldsymbol{\lambda}}^{(k)}) - (\vec{\boldsymbol{\lambda}}_E^{(k+1)} - \vec{\boldsymbol{\lambda}}_E^{(k)})) + \\
& \alpha_2\tau(\mathbb{L}_1 + \mathbb{L}_2)(\hat{\mathbf{z}}^{(k)} - \hat{\mathbf{z}}^{(k-1)}) + \alpha_2\tau(\mathbb{L}_1 + \mathbb{L}_2)(\hat{\hat{Q}}_k - \hat{\hat{Q}}_{k,E})\varepsilon_{tol} + \\
& \alpha_1 \mathbf{F}\left((A^C_{(k-1)}\mathbf{I} - \Lambda^C[\mathbf{f}_E^{(k)}])\mathbf{f}^{(k)} + (\Lambda^C[\mathbf{f}^{(k-1)}] - A^C_{(k-1)}\mathbf{I})\mathbf{f}^{(k-1)}\right) - \\
& \alpha_1 \mathbf{F}\left((A^C_{(k)}\mathbf{I} - \Lambda^C[\mathbf{f}_E^{(k+1)}])\mathbf{f}^{(k+1)} + (\Lambda^C[\mathbf{f}^{(k)}] - A^C_{(k)}\mathbf{I})\mathbf{f}^{(k)}\right) - \\
& \alpha_1 \mathbf{F}\left(\Lambda^C[\mathbf{f}_E^{(k+1)}] - \Lambda^C[\mathbf{f}_E^{(k)}]\right)\mathbf{z}^{(k)}.
\end{aligned}
$$

Proof

Bauer-Fick theorem [6]: $|\lambda(\mathbb{B}) - \lambda(\mathbb{A})| \leq \|\mathbb{B} - \mathbb{A}\|_2$.

$$|\lambda(\mathbb{B})| \geq |\lambda(\mathbb{A})| - \|\mathbb{B} - \mathbb{A}\|_2 \geq \frac{\alpha_1}{\sqrt{1+\beta}} - (1 + 8\alpha_2\tau).$$

$\mathbb{B} := \mathbf{P}^T\mathbf{P} + \alpha_2\tau(\mathbb{L}_1 + \mathbb{L}_2) + \alpha_1\mathbf{F}\Lambda^C[\mathbf{f}_E^{(k+1)}]\overline{\mathbf{F}}^T$;

$\mathbb{A} := \alpha_1\mathbf{F}\Lambda^C[\mathbf{f}_E^{(k+1)}]\overline{\mathbf{F}}^T \sim \alpha_1\Lambda^C[\mathbf{f}_E^{(k+1)}]$: diagonal matrix;

$\lambda(\mathbb{B}), \lambda(\mathbb{A})$: the eigenvalues of $\mathbb{B}, \mathbb{A}$.

Remark

$\mathbb{B} - \mathbb{A} = \mathbf{P}^T\mathbf{P} + \alpha_2\tau(\mathbb{L}_1 + \mathbb{L}_2)$ is diagonal with the elements between $[0, 1 + 8\alpha_2\tau]$.

[6] Bauer F L and Fike C T. Norms and exclusion theorems, Numerische Mathematik,1960.

Proof

$$\left\|\mathbf{z}^{(k+1)}-\mathbf{z}^{(k)}\right\| \leq \frac{\alpha_2\tau}{\frac{\alpha_1}{\sqrt{1+\beta}}-(1+8\alpha_2\tau)}\left\|\mathbf{z}^{(k)}-\mathbf{z}^{(k-1)}\right\|+ \frac{1}{\frac{\alpha_1}{\sqrt{1+\beta}}-(1+8\alpha_2\tau)}\left(\alpha_2\tau\varepsilon_{tol}+\frac{\alpha_1}{\sqrt{\beta^3}}\right). \quad (31)$$

$\alpha_1 > (1+8\alpha_2\tau)\sqrt{1+\beta}$ with small $\tau\varepsilon_{tol} > 0$ and large $\beta > 0$.

$\Downarrow$

$\{\mathbf{z}^{(k)} : k \in \mathbf{N}\}$ is almost convergent.

$\Downarrow$

$\{\mathbf{f}_E^{(k)} : k \in \mathbf{N}\}$ is almost convergent.

Proof

Denote by

$$\mathbf{f}_E^{(k)} \to \mathbf{f}_E, \quad \vec{\boldsymbol{\lambda}}_E^{(k+1)} \to \vec{\boldsymbol{\lambda}}_E, \quad \mathbf{f}^{(k)} \to \mathbf{f}, \quad \vec{\boldsymbol{\lambda}}^{(k+1)} \to \vec{\boldsymbol{\lambda}}$$

as $k \to \infty$.

$$\begin{aligned} & \left(\overline{\mathbf{F}}^T \mathbf{P}^T \mathbf{P} \mathbf{F} + \alpha_1 (\Lambda^C[\mathbf{f}] + \Lambda^C[\mathbf{f}_E])\right)(\mathbf{f} - \mathbf{f}_E) \\ = \; & \alpha_2 (I \otimes D_+, D_+ \otimes I)(\vec{\boldsymbol{\lambda}} - \vec{\boldsymbol{\lambda}}_E) - \\ & \alpha_1 (\Lambda^C[\mathbf{f}_E] - \Lambda^C[\mathbf{f}])\mathbf{f} - \alpha_2 \tau (\mathbb{D}_1 + \mathbb{D}_2) \lim_{k\to\infty} (\tilde{q}_k - \tilde{q}_{k,E}) \varepsilon_{tol}. \quad (32) \end{aligned}$$

Proof

1) By updating process for $\lambda_j^{(k)}$ at each inner iteration:

$$\left\|\boldsymbol{\lambda}^{k,L(k)}\right\|, \left\|\boldsymbol{\lambda}_E^{k,L(k)}\right\| \leq 1, \left\|\mathbf{w}^{(k+1)} - \nabla\mathbf{f}^{(k)}\right\|, \left\|\mathbf{w}_E^{(k+1)} - \nabla\mathbf{f}_E^{(k)}\right\| \leq \varepsilon_{tol},$$

$$\left\|\vec{\boldsymbol{\lambda}}^{(k+1)} - \vec{\boldsymbol{\lambda}}_E^{(k+1)}\right\| \leq C(1+\tau\varepsilon_{tol}).$$

2) Bauer-Fick theorem:

$$\left\|\left(\overline{\mathbf{F}}^T\mathbf{P}^T\mathbf{P}\mathbf{F} + \alpha_1(\Lambda^C[\mathbf{f}] + \Lambda^C[\mathbf{f}_E])\right)^{-1}\right\|_2 \leq \frac{1}{\frac{\alpha_1}{\sqrt{\beta+1}} - 1}.$$

3) $\left\|\Lambda^C[\mathbf{f}] - \Lambda^C[\mathbf{f}_E]\right\| \leq \frac{C}{\sqrt{\beta^3}}\left\|\mathbf{f}-\mathbf{f}_E\right\|.$

Proof

Inserting 1) - 3) into (32).

$$\Downarrow$$

$$\|\mathbf{f}-\mathbf{f}_E\| \leq C\frac{\alpha_1\sqrt{\beta+1}}{\alpha_1-\sqrt{\beta+1}}\left[\frac{1}{\sqrt{\beta^3}}\|\mathbf{f}-\mathbf{f}_E\| + \frac{\alpha_2}{\alpha_1}(1+\tau\varepsilon_{tol})\right].$$

$\alpha_1 > \sqrt{\beta+1}$ with large $\beta > 0$ and small $\tau\varepsilon_{tol}, \alpha_2 > 0$.

$$\Downarrow$$

$$\|\mathbf{f}-\mathbf{f}_E\| \leq C(\alpha_2+\tau\varepsilon_{tol}).$$

Outline

1. Introduction
2. The multi-penalty regularization modeling
3. The alternative iteration scheme
4. Convergence property of iteration process
5. Numerical experiments
6. Summary

Numerical experiments

- Compared with direct method (DM) and RecPF method

Add the additive random noise in the frequency data:

$$\hat{g}^{\delta}_{m',n'} = \hat{f}^{R}_{m',n'} + \delta \times rand(e_{m',n'}) + i \cdot (\hat{f}^{I}_{m',n'} + \delta \times \widetilde{rand}(e_{m,n})).$$

$$\delta = 0.01, \alpha_1 = 10^{-2}, \alpha_2 = 10^{-4}, \tau = 10.$$

C-SMRM: $\beta = 0.5$;

H-SMRM: $\epsilon = 0.1$

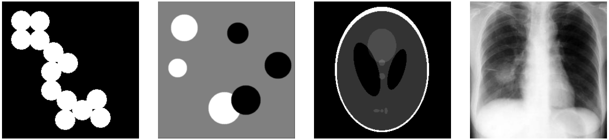

(a) (b) (c) (d)

Figure 3: Object images: $256 \times 256, 512 \times 512, 256 \times 256, 512 \times 512$.

The sampling matrix

- Example 1: random band sampling (RBS)
  256×256: sample 20 rows and 20 columns with $R_{center} = 0.3$ and sampling ratio $R_{total} = 15.02\%$.
  512×512: sample 40 rows and 40 columns with $R_{center} = 0.3$ and sampling ratio $R_{total} = 7.66\%$.
- Example 2: radial sampling
  256×256: sample 22 lines with $R_{total} = 9.36\%$.
  512×512: sample 44 lines with $R_{total} = 9.64\%$.

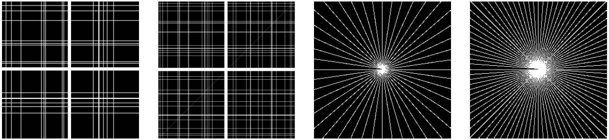

(a) (b) (c) (d)

Figure 4: Masks for RBS and radial sampling.

Example 1: the reconstructed results

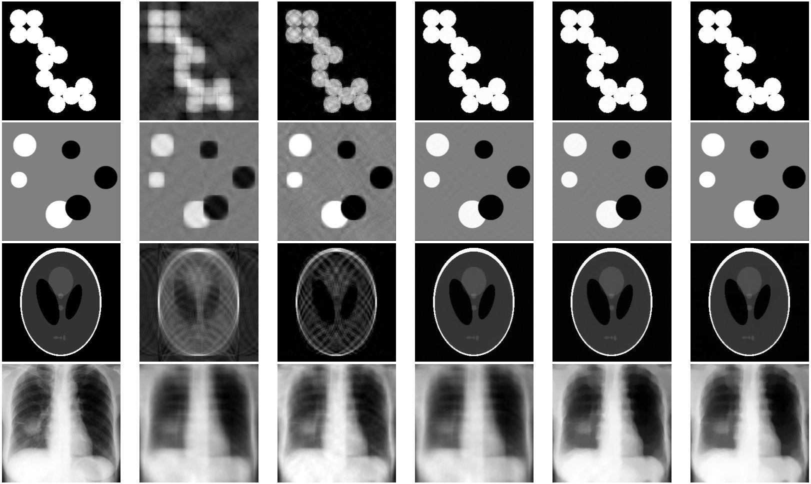

Figure 5: The reconstructed images by random band sampling.

Example 1

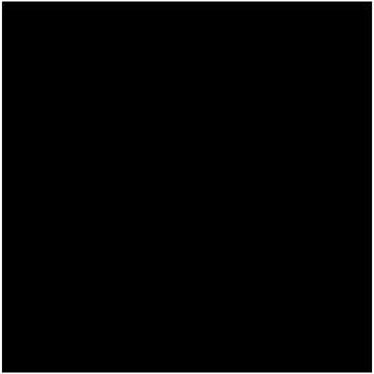

Example 1: the plot of error in C-SMRM, H-SMRM

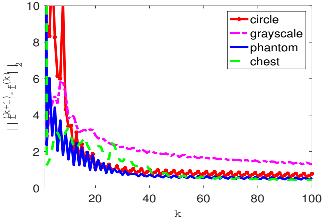

(a) $\|\mathbf{f}^{(k+1)} - \mathbf{f}^{(k)}\|_{l^2}$: $\phi_\beta^C(s)$

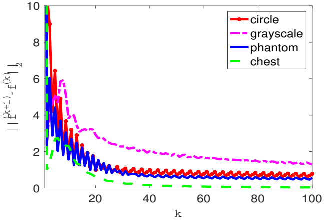

(b) $\|\mathbf{f}^{(k+1)} - \mathbf{f}^{(k)}\|_{l^2}$: $\phi_\epsilon^H(s)$

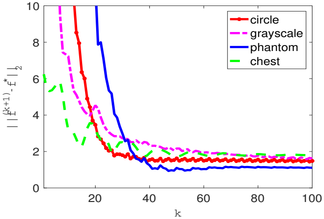

(c) $\|\mathbf{f}^{(k+1)} - \mathbf{f}^{*}\|_{l^2}$: $\phi_\beta^C(s)$

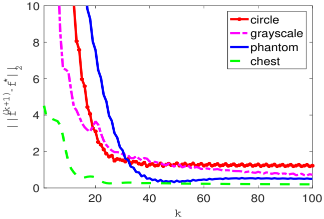

(d) $\|\mathbf{f}^{(k+1)} - \mathbf{f}^{*}\|_{l^2}$: $\phi_\epsilon^H(s)$

Example 1: the test data

Table 1: Computational costs for random band sampling.

image	scheme	ISNR(dB)	ReErr(%)	CPU time(s)	IterNum
circles	DM	3.0437	17.0221	1.5734	40
	RecPF	14.6056	1.0492	**0.2680**	27
	C-SMRM	14.2219	1.1462	1.9248	100
	H-SMRM	**14.7205**	**1.0265**	1.3517	100
grayscale	DM	1.8183	5.7418	9.6594	40
	RecPF	11.9131	0.5245	**1.0943**	21
	C-SMRM	11.5221	0.5627	1.9255	100
	H-SMRM	**13.5264**	**0.2621**	39.1639	100
phantom	DM	1.7383	8.7405	2.1778	40
	RecPF	11.3009	1.9514	**0.3689**	38
	C-SMRM	11.4490	1.8190	1.2895	100
	H-SMRM	**14.4623**	**0.8047**	50.9566	100
chest	DM	2.6484	3.8296	2.1683	40
	RecPF	11.4839	1.0310	**0.2189**	21
	C-SMRM	11.5464	0.9734	1.7518	100
	H-SMRM	**17.4996**	**0.0164**	45.6364	100

Example 2: the reconstructed results

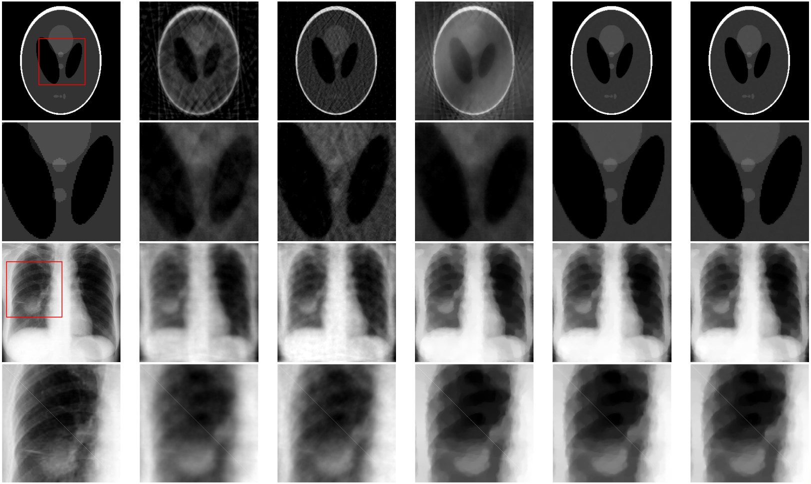

(e) $f^\dagger$ (f) Input (g) DM (h) RecPF (i) C-SMRM (j) H-SMRM

Figure 6: The reconstructions by radial sampling.

Example 2

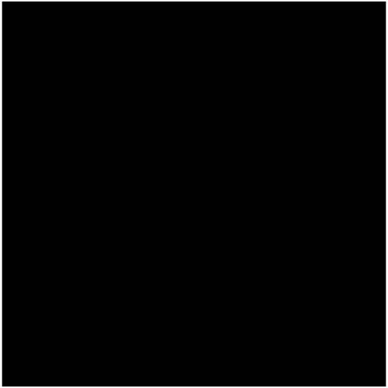

Example 2: the plot of error in C-SMRM, H-SMRM

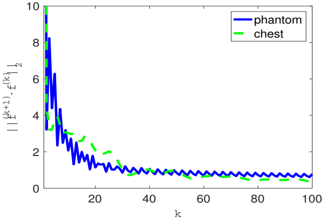

(a) $\|\mathbf{f}^{(k+1)} - \mathbf{f}^{(k)}\|_{l^2}$: $\phi_\beta^C(s)$

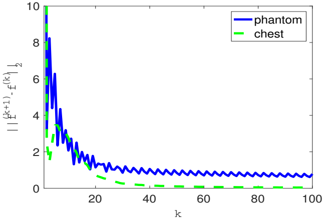

(b) $\|\mathbf{f}^{(k+1)} - \mathbf{f}^{(k)}\|_{l^2}$: $\phi_\epsilon^H(s)$

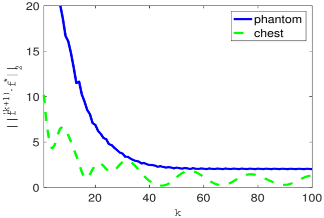

(c) $\|\mathbf{f}^{(k+1)} - \mathbf{f}^{*}\|_{l^2}$: $\phi_\beta^C(s)$

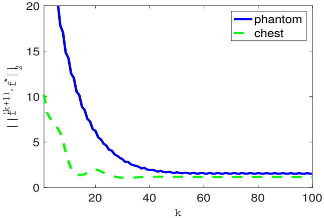

(d) $\|\mathbf{f}^{(k+1)} - \mathbf{f}^{*}\|_{l^2}$: $\phi_\epsilon^H(s)$

Example 2: the test data

Table 2: Computational costs for radial sampling.

image	scheme	ISNR(dB)	ReErr(%)	CPU time(s)	IterNum
phantom	DM	3.8014	11.1883	2.4127	40
	RecPF	12.3966	2.7976	**0.4137**	36
	C-SMRM	12.0596	3.0233	1.3909	100
	H-SMRM	**13.0561**	**2.2250**	45.5967	100
chest	DM	4.0305	4.3061	2.2478	40
	RecPF	2.6372	4.5132	**0.2848**	22
	C-SMRM	11.4866	0.6724	1.3651	100
	H-SMRM	**12.5369**	**3.5845**	37.5576	100

Outline

1. Introduction
2. The multi-penalty regularization modeling
3. The alternative iteration scheme
4. Convergence property of iteration process
5. Numerical experiments
6. Summary

Summary

- To obtain the exact solution in the inner iteration.
- To calculate the approximation iterative solution by solving the diagonal linearized Euler equation in the main loop.
- The convergence of the linearized iteration process is proposed.

Thanks for your attention!